

# Development and Verification of a Series Car Modelica/Dymola Multi-Body Model to Investigate Vehicle Dynamics Systems

Christian Knobel\* Gabriel Janin‡ Andrew Woodruff§

\*BMW Group Research and Technology, Munich, Germany, christian.knobel@bmw.de

‡École Nationale Supérieure de Techniques Avancées, Paris, France, gabriel.janin@ensta.org

§Modelon AB, Lund, Sweden, andrew.woodruff@modelon.se

## Abstract

The development and the verification of a Multi-body model of a series production vehicle in Modelica/Dymola is presented. The model is used to investigate and to compare any possible configuration of actuators to control vehicle dynamics with a general control approach based on model inversion and a non-linear online optimization.

*Keywords: Multi-body Vehicle Model, Vehicle Dynamics, Model Verification, Model Validation, Active Vehicle Dynamics Systems, Tire Model, Suspension Kinematics, Suspension Compliance*

## 1 Introduction

Systems for control of Vehicle Dynamics went to series production for the first time in 1978 with the limitation of brake pressure to avoid locking the wheels to ensure cornering under all braking conditions. Braking individual wheels (independently from the drivers commands) to stabilize the vehicle at the driving limit went to series production in 1995. In the last few years, control systems for vehicle dynamics with additional actuators to control steering, drive torque distribution and wheel load distribution have entered the market.

All of these systems acting on the force allocation from the center of gravity (CG) to the four tire contact patches (TCP) and on the force transfer at the TCPs. This strong interdependence between these systems<sup>1</sup> is the reason why independent operation of more than one of them is only possible with a loss of potential to prevent critical interferences. In [2] (cf. also [3], [4], [5], [6] and [7]) a general approach was introduced to investigate the ref-

<sup>1</sup>cf. [1] for an overview and a detailed classification of systems for vehicle motion control.

erence behavior (best possible allocation and transfer of forces acting on the vehicle) for any configuration of actuators controlling vehicle dynamics including all steering angles  $\delta = [\delta_1 \ \delta_2 \ \delta_3 \ \delta_4]^T$ , brake/drive torques  $M = [M_1 \ M_2 \ M_3 \ M_4]^T$ , wheel loads  $F_z = [F_{z1} \ F_{z2} \ F_{z3} \ F_{z4}]^T$  and even camber angles  $\gamma = [\gamma_1 \ \gamma_2 \ \gamma_3 \ \gamma_4]^T$ . The comparison of the reference operation of different configurations may support decisions in the future development of vehicle dynamics. The investigation of the reference behavior also supports controller development and the dynamic specification of the actuators, or makes it possible to investigate the potential loss if the applied actuators have less dynamics compared to the ideal required dynamics. The reconfigurable behavior of the general approach allows further investigation of the impact of actuator failures on vehicle dynamics for reliability investigations.

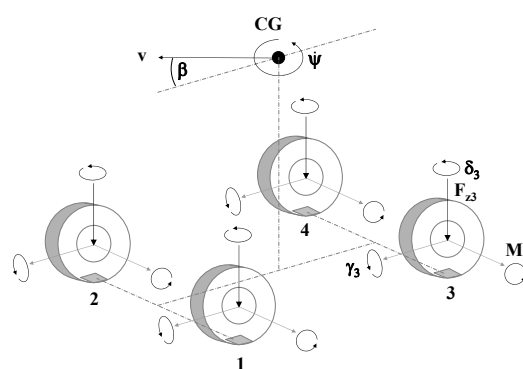


Figure 1: Planar vehicle model with influencing variables and vehicle motion  $y$

Because the approach presented in [2] is based on model inversion of a plane vehicle model with the plane motion  $y = [\psi \ \beta \ v]^T$  described by the yaw rate  $\dot{\psi}$ , the body slip angle  $\beta$  and the velocity  $v$  (cf. Figure 1), a verified multi-body model is needed as ve-

hicle model to ensure that the control approach works also with all effects neglected during the controller design. Using the verified Modelica/Dymola Multi-body vehicle model presented in this paper as a vehicle model for the control approach allows investigation and comparison of all possible configurations of available actuators quickly and easily.

The possibility to model multi-body suspension assemblies, controllers, hydraulic and mechatronic actuators in one and the same environment was the reason to choose Dymola as the modeling and simulation tool. Development and verification of the model was done bottom-up. Multi-body front and rear suspension, tires, steering system, power train and the body were modeled and then verified separately with test rig results as shown in Section 2. Creating the multi-body vehicle model by connecting those subsystems together is presented in Section 3 as well as the verification process of the full vehicle through objective test maneuvers with a series car equipped with additional measurement technology. Finally, an application example is presented in Section 4.

## 2 Development and Verification of Subsystems

Using the Multi-Body Library [8] and the Vehicle Dynamics Library [9], tire, suspension, body and environment for the multi-body model were constructed. Simple models for the steering and the power train system are developed only for the verification of the multi-body vehicle model with a conventional series production vehicle.

### 2.1 Tire

Pacejka's Magic Formula [10] is used to model the plane transfer behavior of the tire, which calculates first the pure forces

$$\begin{aligned} F'_{xoi} &= D \sin(C \arctan(B\kappa - E(B\kappa - \arctan B\kappa))) \\ F'_{yoi} &= D \sin(C \arctan(B\alpha - E(B\alpha - \arctan B\alpha))) \end{aligned} \quad (1)$$

$i \in \{1 \dots 4\}$  designated with ' to indicate the representation with the wheel coordinate system out of the inputs longitudinal slip  $\kappa$ , tire side slip angle  $\alpha$ , wheel load  $F_z$  and camber angle  $\gamma$ . Secondly,

$$\begin{aligned} F'_{xi} &= F'_{xoi} \cos(C \arctan(B\alpha - E(B\alpha - \arctan B\alpha))) \\ F'_{yi} &= F'_{yoi} \cos(C \arctan(B\kappa - E(B\kappa - \arctan B\kappa))) \end{aligned} \quad (2)$$

the interdependence between the longitudinal and lateral tire forces is considered where the peak parameter  $D(F_z, \gamma)$ , the shape parameter  $C$ , the stiffness parameter  $B(F_z, \gamma)$  and the curvature parameter  $E(F_z, \gamma)$  are different for (1), (2) and for longitudinal and lateral directions, respectively. For the identification of these parameters, an error minimization is used to fit the model result to the test rig results of the tire used (cf. Figure 2 and Figure 3). Because braking (negative longitudinal tire forces) is more important for vehicle dynamics control than accelerating (positive longitudinal tire forces), different weighting factors are used to get a better correlation of the negative longitudinal tire forces.

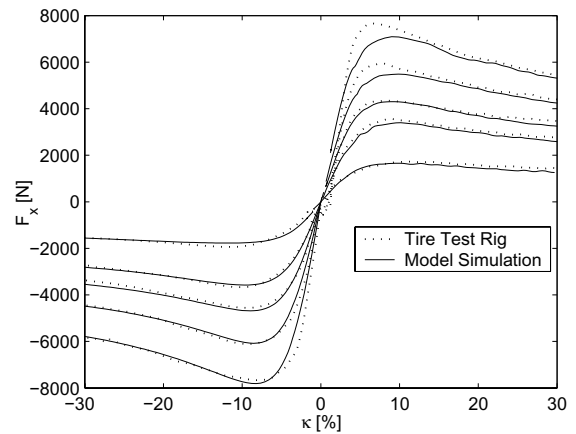


Figure 2: Longitudinal force  $F_x$  over longitudinal slip  $\kappa$  for different wheel loads  $F_z$

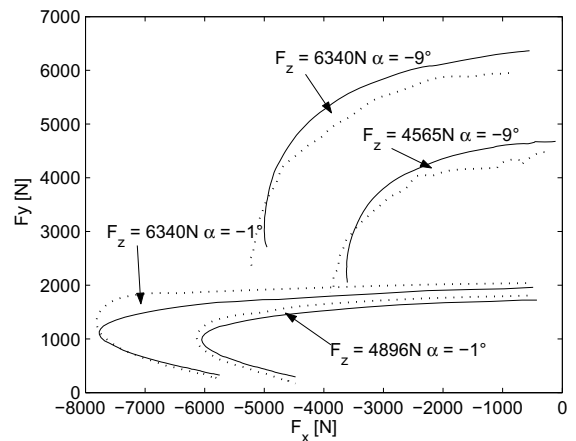


Figure 3: Lateral force  $F_y$  over longitudinal force  $F_x$  (longitudinal slip  $\kappa$  sweeps at different tire side slip angles  $\alpha$  and wheel loads  $F_z$ ) known as a Krempel Graph

## 2.2 Suspension

For the front and rear suspension, ADAMS models could be used as source to model the McPherson front suspension (cf. Figure 4) and the semi-trailing

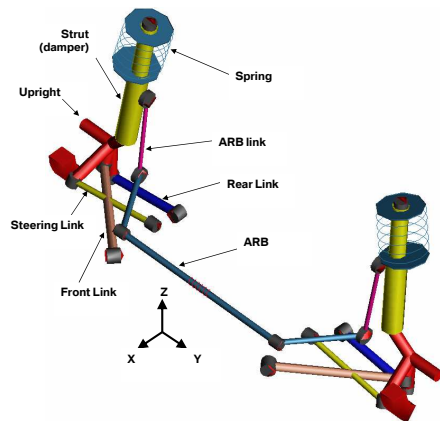


Figure 4: McPherson front suspension design

arm rear suspension design (cf. Figure 5) in Modelica/Dymola.

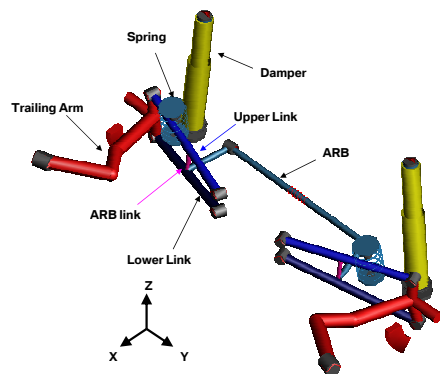


Figure 5: Semi-trailing arm rear suspension design

The default models for those suspension designs in the Vehicle Dynamics Library [9] could not be used without customizing and modifying the design, the joint location and the kinematic relationships to match the behavior of the source models in ADAMS.

The McPherson front suspension used independent lower rods instead of the conventional control arm in [9]. The rear suspension used a trailing arm design with two guiding links, and the body spring and anti-roll subsystems were attached to the upper guiding link (cf. [11]). Non-linear bump stops were added on the damper's tube of the front and rear suspension.

The hard points for all joint locations of the model need to be adjusted to agree with the ADAMS source model.

The kinematics of the suspension models are verified using a vertical travel sweep test rig which needs to be modeled in Modelica/Dymola as well. Camber and toe changes are plotted to verify the kinematic behavior of the suspension models with the source model and the real suspension of the used series vehicle (cf. Figure 6).

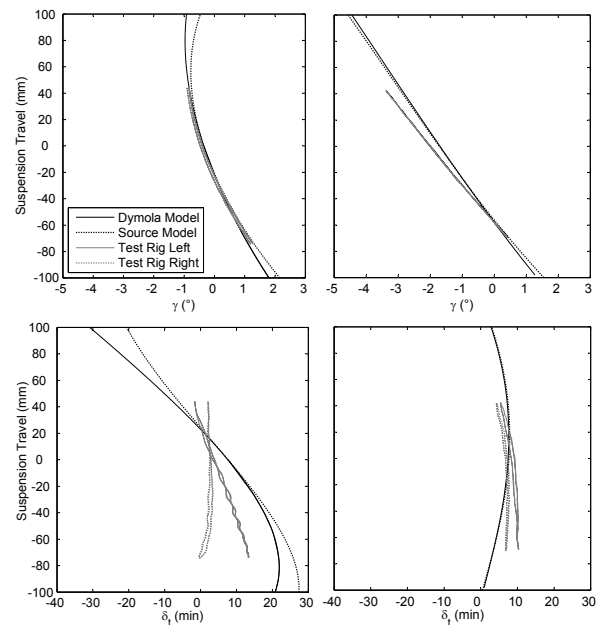


Figure 6: Kinematic analysis: camber in degrees and toe in angular minutes for front (left) and rear suspension (right)

Simulation of the rigid suspension model (without any bushings) was impossible and caused singularity errors. After the implementation of bushings, simulation of the multi-body front and rear suspensions was possible. However, a pure investigation of the rigid kinematics was only possible using very stiff bushings, which is the reason for the differences between the source model and the Modelica/Dymola model in Figure 6.

The kinematics of the real suspension could only be verified with bushings, which is again the main reason for the differences between the model results and the real test rig results shown in Figure 6.

## 2.3 Further Subsystems of the Vehicle

After modeling the tires and suspensions, adding body, power train and steering system models, as well as the vehicle's environment, is necessary to the complete multi-body vehicle model.

The vehicle's body is considered to be rigid and its mass is distributed as follows: one summarized sprung

mass, including the driver, one passenger and fuel is in the body whereas the unsprung mass of the wheels including brake caliper and rotor and their links is distributed to the four wheels. The vehicle's inertias at the CG are identified on a pendulum test rig.

The complexity and accuracy of the power train and steering models are rather low because they are only used to get reasonable connections between the driver's inputs and the brake/drive torques  $M$  and the wheel steer angles  $\delta$ . The former uses a speed controller and a differential gear to distribute the torques to the four wheels similar to the series production vehicle. The latter consists a rack-and-pinion steering system including a rotational spring in the steering shaft.

The study of a full-vehicle model requires the modeling of its environment. The equations of motion can only be solved by having a complete description of physical system. Therefore, the interaction between the vehicle and the world must be taken into account. It consists the interactions between vehicle and driver, vehicle and air, and tire and road. The road is modeled by a flat surface with with a road friction coefficient  $\mu$ . The aerodynamic drag force  $F_x^{aero} = -\frac{1}{2}\rho c_x v^2$  applied at the center of gravity simplifies the interaction between air and vehicle. These environments are from the Vehicle Dynamics Library [9]. Only driver models need to be built up to be able to simulate the objective test maneuvers for the verification in Section 3.

The active control actuators are modeled by ideal revolute joints inserted at the rigid connection between the suspension and wheel subsystems. This meant the wheels could be manipulated directly and without altering the suspension geometry. Passive systems are represented by constant values as inputs for the ideal actuators.

### 3 Development and Verification of the Multi-body Vehicle Model

Connecting the subsystems from Section 2 creates the multi-body vehicle model.

Important steps are the definition, design and implementation of the model. A more important step is to check if the model matches real vehicle behavior. Therefore, the vehicle and the model behavior are compared with objective test maneuvers such as steady state cornering (steady state behavior), steering steps (dynamic behavior in the time domain) and sine-sweeps (dynamic behavior in the frequency domain). Body side slip angle  $\beta$  and velocity  $v$  are measured using an optical Correvit sensor, roll  $\phi$  and pitch  $\theta$

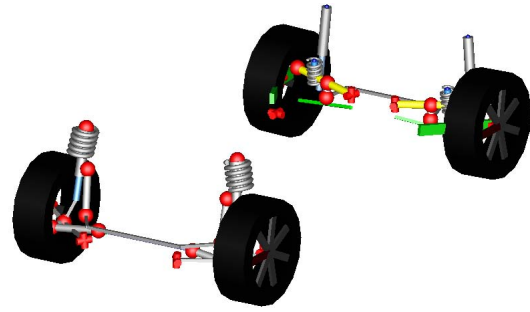


Figure 7: Chassis representation of the multi-body vehicle model

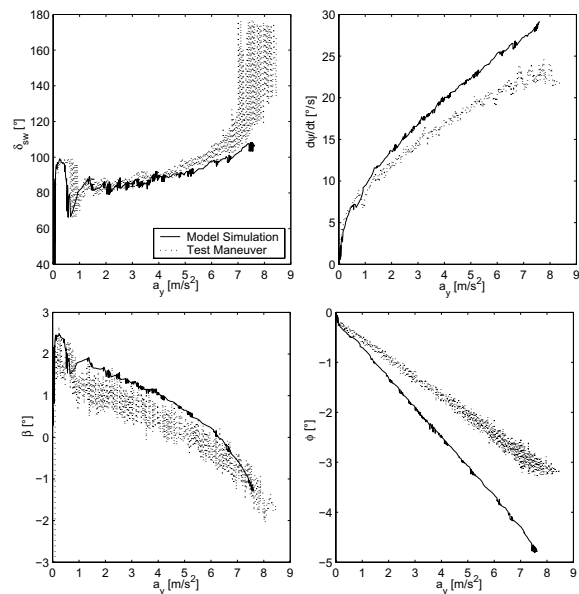
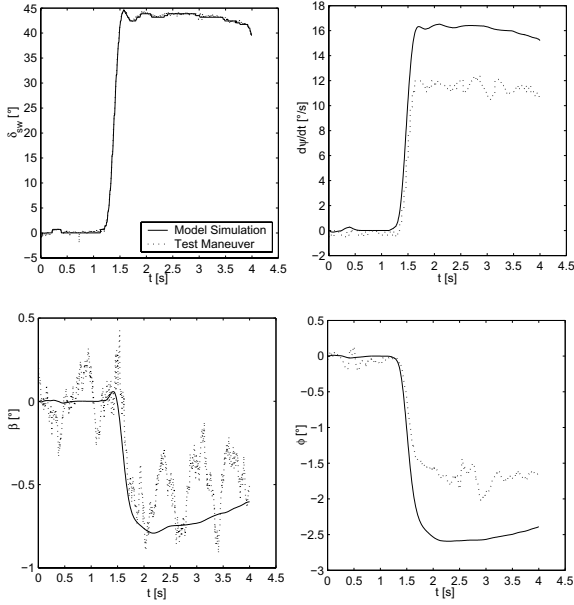


Figure 8: Steady state cornering,  $r=40m$ , dry road  $\mu=1$

are measured indirectly by suspension travel sensors at all four wheels, and all translational accelerations  $a_x, a_y, a_z$  as well as the rotational rates  $\dot{\psi}, \dot{\phi}, \dot{\theta}$  are measured by a sensor cluster located at the CG. The steering wheel angle  $\delta_{sw}$  and the steering wheel torque  $M_{sw}$  are measured using an instrumented steering wheel.

The results of the verification without any fitting of uncertain parameters like stiffness of the bushings, or friction coefficient  $\mu$  of the road are presented in Figure 8 and Figure 9.

The main reason for the higher yaw rate generated by the model in both maneuvers is the uncertain road friction coefficient  $\mu$ . The higher roll in both maneuvers is caused by different stiffnesses of the body springs used in the model and the real vehicle.


 Figure 9: Step steer,  $v=70$  km/h, dry road  $\mu=1$ 

## 4 Application of the Model

Exchanging the conventional steering and power train system of the verified vehicle model and using the ideal actuators as described in 2.3 leads to a generic configuration for vehicle dynamics control. All steering angles  $\delta$ , drive/brake torques  $M$ , wheel loads  $F_z$  and camber angles  $\gamma$  (cf. Figure 1) could be used passively or actively controlled by the general allocation approach presented in [2]. A non-linear online optimization calculates the arbitrary parameters for the under determined inverses of the over-actuated<sup>2</sup> plane motion vehicle model (cf. 1). The number of the arbitrary parameters depends on the available actuators for the influencing variables. These arbitrary parameters are always used by the non-linear online optimization to minimize the maximum adhesion potential utilization

$$\eta_i^2 = \left( \frac{F_{xi}}{F_{xi\max}} \right)^2 + \left( \frac{F_{yi}}{F_{yi\max}} \right)^2 \quad (3)$$

( $0 \leq \eta_i \leq 1$ ) of the four tires  $i \in \{1 \dots 4\}$  is approximated by an elliptic relation. The forces  $F_{xi\max}$  and  $F_{yi\max}$  depend on the wheel load  $F_{zi}$  and the camber angles  $\gamma_i$ . The control commands out of these optimization are used as inputs for the multi-body vehicle (cf. Figure 10). Inputs for the optimization are the torque and forces  $u = [M_{zCG} \ F_{xCG} \ F_{yCG}]^T$  acting on the center of gravity. The allocation of these forces to the TCPs and the force transfer in the TCPs are optimized

<sup>2</sup>cf. [12] for definition and examples

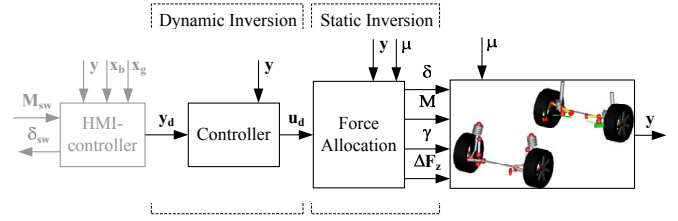


Figure 10: Control loop with the multi-body vehicle model

with the optimization objective

$$\min \max \eta_i \quad (4)$$

This setup facilitates investigation into the reference behavior (best possible allocation and transfer of forces acting on the vehicle) of the vehicle dynamics for every configuration of available actuators influencing vehicle dynamics for the verified multi-body vehicle model.

Changing the number of available actuation during a driving maneuver allows investigation into the impact of actuator failures on vehicle dynamics, which may support reliability investigations of active vehicle dynamics systems.

Such an investigation is presented as an exemplary application of the presented multi-body vehicle model (cf. Figure 11, Figure 12 and Figure 13). The front right steering actuator of a vehicle (equipped with four steering actuators, four drive torque actuators and four actuators to control the wheel load distribution) fails. The failure occurs after one second of driving an open loop single lane change at a constant speed  $v=70$  km/h (cf. Figure 13). All actuators and actuator dynamics are limited for the optimization (4) to values of actual available actuators. The actuator fails in the worst case situation at maximum steering angle of  $\delta = 1.8$  degrees and is assumed to be self-locked after the failure occurred. To compensate this fixed steering error, the vehicle exhibits the same amount of body slip angle as can be seen in Figure 13. Steering back to straight driving again the failure wheel becomes the outer wheel (with respect to the center of the corner) with more wheel load. Therefore, the optimization reduces the wheel load at this wheel as much as possible. However, the steering angles and drive torques at the other wheels are much higher compared to the usual driving condition without failure (right side of Figures 11, 12 and 13). The maneuver presented is close to the physical driving limit since two tires have already reached their maximum possible adhesion potential utilization (cf. Figure 12). The lateral acceler-

ation  $a_y$  is reaching  $4 \text{ m/s}^2$  at the minimum and maximum of the yaw rate  $\psi$ . This performance meets the actual specification of flat run-flat tires.

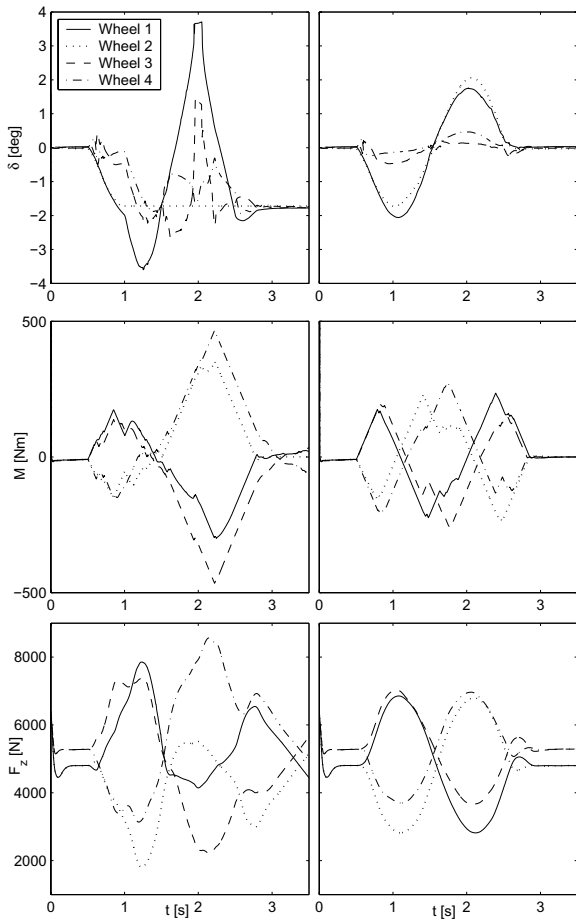


Figure 11: Influencing variables of vehicle with steering actuator failure (left) and usual working vehicle (right)

## 5 Conclusion and Outlook

The development and the verification of a multi-body model of a series production vehicle is presented. This vehicle model was used to investigate and compare any possible configuration of actuators to control vehicle dynamics. In this context, Modelica/Dymola has proven to be a practical environment for future development of vehicle models including mechatronic and hydraulic actuators, multi-body suspensions and controllers. To develop, verify and use Modelica/Dymola models in an efficient way, however, interfaces to CAD systems to import CAD model data and interfaces to real time environments are desirable. Especially for this project, a library for non-linear optimization was missed, which was the reason why

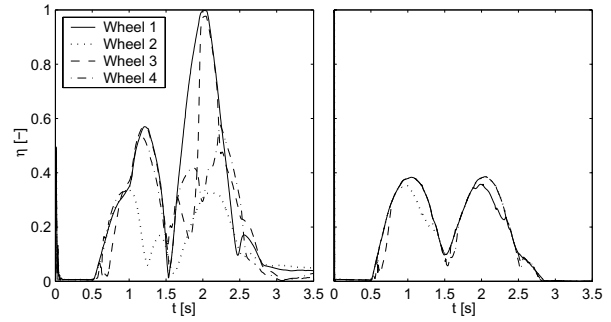


Figure 12: Adhesion potential utilization of failure (left) and usual vehicle (right)

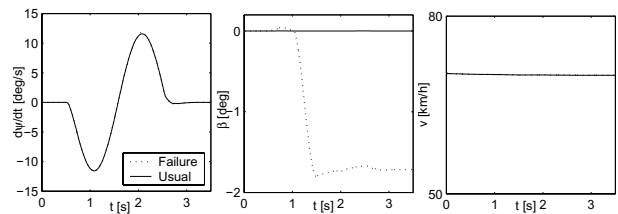


Figure 13: Plane vehicle motion of the vehicle with steering actuator failure (-) and usual working vehicle (:)

this part of the presented control approach was realized in MATLAB/Simulink. The presented Modelica/Dymola multi-body model was implemented into MATLAB/Simulink using the Simulink Interface of Dymola.

The outlook of the presented project is to improve the matching of the model by using an error minimization. Parameters for the error minimization are probably the uncertain stiffness of the bushings and the road friction coefficient  $\mu$ .

The presented example of steering actuator failure could be improved by adding a strategy of actively controlled camber (assuming the availability of such a system) for steering actuator failures which counteracts the failure force generated by the tire side slip angle  $\alpha_i$  of the failure wheel.

## References

- [1] J. Andreasson, C. Knobel, and T. Bunte. On Road Vehicle Motion Control - striving towards synergy. In *Proc. of 8th International Symposium on Advanced Vehicle Control AVEC*, 2006.
- [2] C. Knobel, A. Pruckner, and T. Bunte. Optimized Control Allocation - A General Approach to Control and to Investigate the Motion of Over-

- actuated Vehicles. Submitted paper for 4th IFAC Symposium on Mechatronic Systems, 09 2006.
- [3] Y. Hattori, K. Koibuchi, and T. Yokoyama. Force and Moment Control with Nonlinear Optimum Distribution for Vehicle Dynamics. In *Proc. of 6th International Symposium on Advanced Vehicle Control AVEC*, 2002.
- [4] E. Ono, Y. Hattori, Y. Muragishi, and K. Koibuchi. Vehicle Dynamics Control Based on Tire Grip Margin. In *Proc. of 7th International Symposium on Advanced Vehicle Control AVEC*, 2004.
- [5] R. Orend. Steuerung der Fahrzeugbewegung mit minimaler Kraftschlussausnutzung an allen vier Rädern. In *Proc. of Steuerung und Regelung von Fahrzeugen und Motoren - Autoreg. VDI*, 2004.
- [6] J. Andreasson and T. Bunte. Global Chassis Control Based on Inverse Vehicle Dynamics Models. Presented at XIX IAVSD World Congress, 10 2005.
- [7] T. Bunte and J. Andreasson. Integrierte Fahrwerkregelung mit minimierter Kraftschlussausnutzung auf der Basis dynamischer Inversion. In *Proc. of Steuerung und Regelung von Fahrzeugen und Motoren - Autoreg, Wiesloch*, 2006.
- [8] M. Otter, H. Elmqvist, and S. E. Mattsson. The New Modelica MultiBody Library. In *Proc. of the 3. International Modelica Conference*, pages 311–330, 2003.
- [9] J. Andreasson. Vehicle dynamics library. In *Proc. of the 3rd International Modelica Conference*. Modelica Association, 2003.
- [10] H. B. Pacejka. *Tyre and Vehicle Dynamics*. Butterworth-Heinemann, Oxford, 2002.
- [11] A. Woodruff. Camber Prevention Methods using a Modelica/Dymola Multi-body Vehicle Model. Master's thesis, Mechanical and Materials Engineering Department, Queen's University, Kingston, ON, Canada, 2006.
- [12] M. Valášek. Design and Control of Under-Actuated and Over-Actuated Mechanical Systems - Challenges of Mechanics and Mechatronics. *Vehicle System Dynamics*, 40:37–50, 2003.